Spontaneous heavy cluster emission rates using microscopic potentials

D. N. Basu*
Variable Energy Cyclotron Centre, 1/AF Bidhan Nagar, Kolkata 700 064, India
(Received 8 March 2002; published 1 August 2002)

The nuclear cluster radioactivities have been studied theoretically in the framework of a microscopic superasymmetric fission model (MSAFM). The nuclear interaction potentials required for binary cold fission processes are calculated by folding in the density distribution functions of the two fragments with a realistic effective interaction. The microscopic nuclear potential thus obtained has been used to calculate the action integral within the WKB approximation. The calculated half-lives of the present MSAFM calculations are found to be in good agreement over a wide range of observed experimental data.

DOI: 10.1103/PhysRevC.66.027601 PACS number(s): 23.70.+j, 24.75.+i, 25.85.Ca

Since the first experimental observation of cluster radioactivity [1], a lot of effort, both experimental and theoretical, has gone into the understanding of the physics of cluster radioactivity. Lifetimes of the cluster radioactivities of radioactive nuclei have been predicted theoretically using various models and compared with existing experimental data from time to time. These models can be broadly classified as the superasymmetric fission model (SAFM) [2–4] and the preformed cluster model (PCM) [5]. In the SAFM the barrier penetrabilities are calculated assuming two asymmetric clusters. In the PCM the cluster is assumed to be formed before it penetrates the barrier and its preformation probability is also included in the calculations. Though the physics of the two approaches is apparently different, but actually they are almost similar. Interpreting the cluster preformation probability within a fission model as the penetrability of the prescission part of the barrier, it was shown that the PCM is, in fact, equivalent to the fission model [6]. However, the PCM has been found to be better applicable for lighter clusters while SAFM is more apt for all cluster decays [7].

Both the theoretical approaches described above use either phenomenological potentials or the proximity-type potentials to calculate nuclear interaction between the two fragments. The SAFM calculations using proximity-type potentials or semiempirical heavy ion potentials obtained by fitting the elastic scattering data or other phenomenological nuclear potentials for interaction between the fragments do not reproduce the observed cluster radioactivity lifetimes successfully. The SAFM using a parabolic potential approximation for the nuclear interaction potential, which is a rather unusual fragment interaction potential, however, has been found to provide reasonable estimates for the lifetimes of cluster radioactivity [4]. The PCM with various nuclear potentials have also been tried with some success for the α radioactivity but was not much successful even for a very limited number of heavier cluster decays. In the present work microscopically calculated nuclear interaction potentials have been used in the SAFM approach with reasonable success for calculating the lifetimes of cluster radioactive decays over a wide range of emitted heavy clusters from a large number of parent nuclei. The microscopic nuclear potential obtained by double folding the cluster density distributions with realistic effective interaction is also very fundamental in nature. Moreover, the use of global microscopic nuclear potentials over a wide range of daughter and emitted cluster interactions is also aesthetically appealing.

In the SAFM the half-life of the parent nucleus against the split into a cluster and a daughter is calculated using the WKB barrier penetration probability. The assault frequency ν is obtained from the zero-point vibration energy $E_v = (1/2)\hbar\omega = (1/2)h\nu$. The half-life T of the parent nucleus (A,Z) against its split into a cluster (A_e,Z_e) and a daughter (A_d,Z_d) is given by

$$T = [(h \ln 2)/(2E_v)][1+\exp(K)], \tag{1}$$

where the action integral K within the WKB approximation is given by

$$K = (2/\hbar)\int_{R_a}^{R_b}[2\mu(E(R)-E_v-Q)]^{1/2}dR. \tag{2}$$

Here $\mu = mA_eA_d/A$ is the reduced mass, m is the nucleon mass, and $E(R)$ is the total interaction energy of the two fragments separated by the distance R between the centers, which is equal to the sum of nuclear interaction energy, Coulomb interaction energy, and the centrifugal barrier. The amount of energy released in the process is Q and R_a and R_b are the two turning points of the WKB action integral determined from the equations,

$$E(R_a) = E(R_b) = Q + E_v\,. \tag{3}$$

Energetics allow spontaneous emission of cluster only if the released energy

$$Q = M - (M_e + M_d) \tag{4}$$

is a positive quantity, where M, M_e, and M_d are the atomic masses of the parent, the emitted cluster and the daughter nuclei, respectively, expressed in the units of energy. Correctness of predictions for possible decay modes therefore rests on the accuracy of the ground state masses of nuclei while the reliability of the half-life calculations requires proper zero-point vibration energies and nuclear interaction energies.

*Email address: dnb@veccal.ernet.in

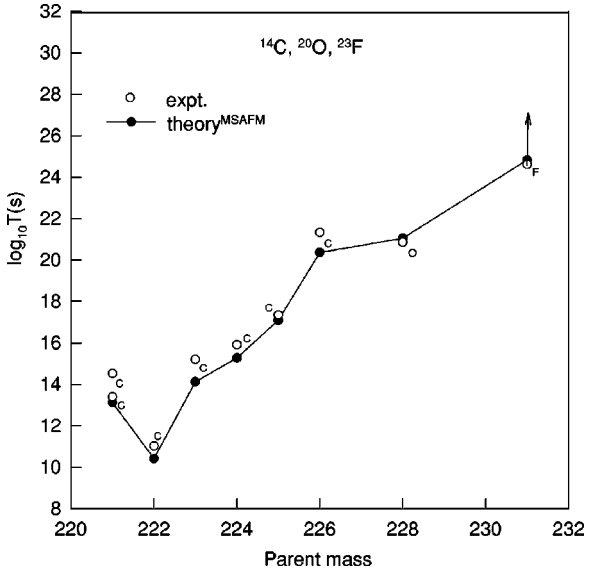

FIG. 1. Logarithmic half-lives for carbon, oxygen, and fluorine cluster decays plotted against parent mass number. The continuous line connects the calculated values. The experimental data are shown by open circles, and the arrow attached to one point indicates that this is only the lower limit determined experimentally.

In the present work the total interaction energy $E(R)$ has been evaluated using microscopic nuclear potential along with the Coulomb potential over the entire domain of interaction. The microscopic nuclear potentials have been obtained by double folding in the densities of the fragments with the finite range realistic $M3Y$ effective interacion as

$$V(R)=\int\int \rho_1(\vec{r}_1)\rho_2(\vec{r}_2)v[|\vec{r}_2-\vec{r}_1+\vec{R}|]d^3r_1d^3r_2. \quad (5)$$

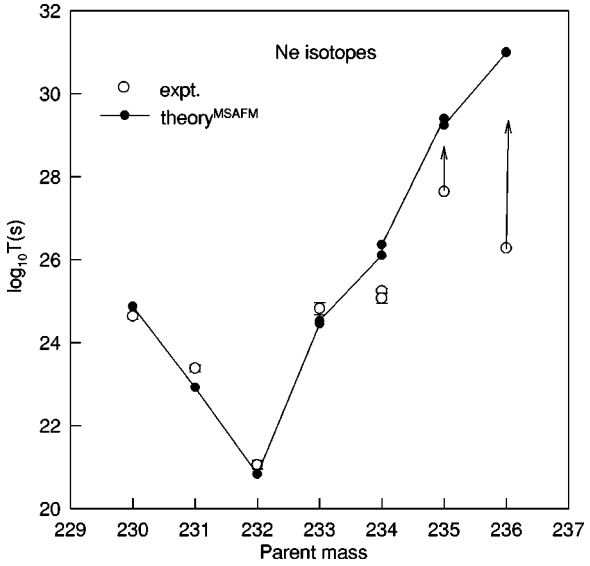

FIG. 2. Plot of logarithmic half-lives for cluster decays by neon emission versus parent mass number. The continuous line connects the calculated values for different isotopes of neon. The experimental data are shown by open circles, and the arrows attached to two points indicate that these are only lower limits determined experimentally.

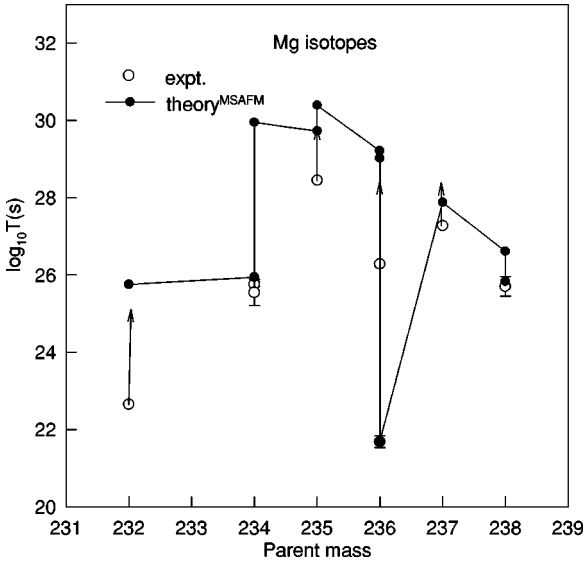

FIG. 3. Same as Fig. 2 but for magnesium isotopes.

The density distribution used for the clusters has been chosen to be of the spherically symmetric form given by

$$\rho(r)=\rho_0/\{1+\exp[(r-c)/a]\}, \quad (6)$$

where

$$c=R(1-\pi^2a^2/3R^2), \quad R=1.13A^{1/3}, \quad \text{and} \quad a=0.54 \text{ fm} \quad (7)$$

and the value of ρ_0 is fixed by equating the volume integral of the density distribution function to the mass number of the cluster. The finite range $M3Y$ effective interaction $v(s)$ appearing in the Eq. (5) is given by [8]

$$v(s)=7999.0\exp(-4s)/(4s)-2134.0\exp(-2.5s)/(2.5s). \quad (8)$$

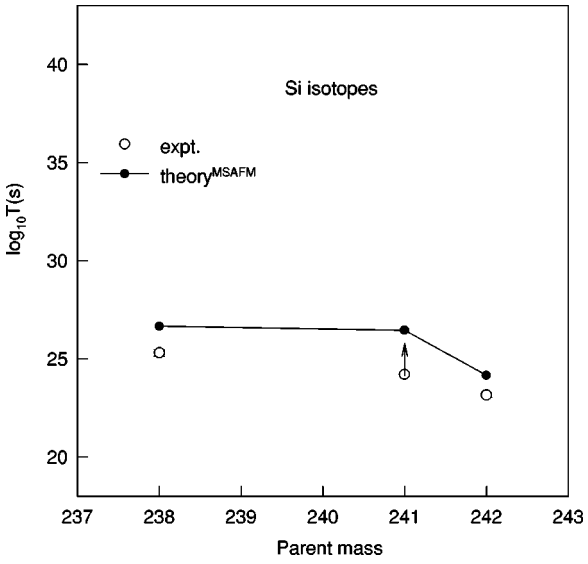

FIG. 4. Same as Fig. 2 but for silicon isotopes.

TABLE I. Comparison between measured and calculated half-lives.

Parent		Daughter		Emitted		ASAFM 1986	ASAFM 1991	MSAFM	Expt.
Z	A	Z_d	A_d	Z_e	A_e	$\log_{10}T(s)$	$\log_{10}T(s)$	$\log_{10}T(s)$	$\log_{10}T(s)$
87	221	81	207	6	14	15.00	14.37	13.39	14.52
88	221	82	207	6	14	13.83	14.25	13.12	13.39
88	222	82	208	6	14	12.56	11.16	10.41	11.02
88	223	82	209	6	14	14.78	15.20	14.12	15.20
88	224	82	210	6	14	17.39	15.95	15.27	15.90
89	225	83	211	6	14	18.45	17.80	17.09	17.34
88	226	82	212	6	14	22.44	20.97	20.36	21.33
90	228	82	208	8	20	22.44	21.95	21.05	20.86
90	230	80	206	10	24	24.86	25.27	24.87	24.64
91	231	81	207	10	24	21.98	23.38	22.92	23.38
92	232	82	208	10	24	20.41	20.81	20.83	21.06
92	233	82	209	10	24	23.11	24.80	24.45	24.82
92	233	82	208	10	25	23.44	25.16	24.53	24.82
92	234	82	210	10	24	25.72	26.13	26.11	25.25
92	234	82	208	10	26	26.16	27.05	26.36	25.07
92	234	80	206	12	28	24.56	25.03	25.94	25.75
92	234	80	204	12	30	29.15	29.64	29.95	25.54
94	236	82	208	12	28	19.79	20.26	21.70	21.68
94	238	82	210	12	28	24.81	25.29	26.61	25.70
94	238	82	208	12	30	24.42	24.91	25.83	25.70
94	238	80	206	14	32	23.69	24.23	26.66	25.30
96	242	82	208	14	34	20.75	21.31	24.16	23.15
91	231	82	208	9	23	24.74	25.89	24.82	>24.61
92	235	82	210	10	25	28.31	30.05	29.40	>27.64
92	235	82	209	10	26	28.40	30.17	29.24	>27.64
92	236	82	212	10	24	30.51	30.93	30.99	>26.28
92	236	82	210	10	26	30.76	31.65	31.00	>26.28
92	232	80	204	12	28	24.46	24.93	25.75	>22.65
92	235	80	207	12	28	27.33	29.30	29.72	>28.45
92	235	80	205	12	30	28.47	30.51	30.39	>28.45
92	236	80	208	12	28	27.82	28.29	29.21	>26.28
92	236	80	206	12	30	28.09	28.58	29.02	>26.28
93	237	81	207	12	30	25.84	27.55	27.88	>27.27
95	241	81	207	14	34	22.45	24.41	26.44	>24.20

For the direct part of the $M3Y$ effective interaction the long range one-pion exchange potential is exactly equal to zero. As the cluster decays involve only very low energies, the finite range exchange interaction has not been considered because it is important only at higher energies [9]. This microscopic nuclear potential energy is then used to calculate the total interaction energy $E(R)$ for use inside the WKB action integral. The two turning points of the action integral have been obtained by solving Eq. (3) using microscopic double folding potential given by Eq. (5) along with the Coulomb potential. Then the WKB action integral between the two turning points has been evaluated numerically for calculating the half-lives of the cluster decays. The zero-point vibration energies used in the present calculations are same as that described by Eqs. (5) in Ref. [10]. The shell effects for every cluster radioactivity are implicitly contained in the zero-point vibration energy due to its proportionality with the Q value, which is maximum when the daughter nucleus has a magic number of neutrons and protons. A normalization factor of 0.9 for the microscopic nuclear potential has been used to obtain the optimum fit. The present calculation uses the experimental ground state masses for calculating the released energy Q. Whenever the experimental ground state masses are not available, it uses the theoretically calculated ground state masses from the latest mass table [11].

It is important to mention here that in the analytical superasymmetric fission model (ASAFM) [2] calculations, the entire interaction region is divided into two distinct zones. In the overlapping zone, where the distances of separation between the centers of the two fragments are below the touching radius, a parabolic form for the nuclear interaction potential has been used. And for distances beyond the touching

radius only the Coulomb potential plus the centrifugal barrier for the separated fragments have been considered within a framework of a liquid drop model two center spherical parametrization. Treating the region beyond the touching radius as a nuclear force free-zone and approximating the nuclear interaction potential to a parabolic form in the overlapping region yield analytical expression for the WKB action integral [2]. Although the overall uncertainty of this ASAFM was found to be small, neither the division of the interaction region into two distinct domains is justifiable nor the use of parabolic nuclear potential has much physical basis.

In Figs. 1, 2, 3, and 4 the experimental data for logarithmic half-lives [4,12–19] have been plotted against the mass numbers of parent nuclei along with the results of the present calculations for zero angular momentum of the fragments. In all the figures, the open circles depict the experimental data while the continuous line with solid circle represents the present calculations [microscopic superasymmetric fission model (MSAFM)]. The upward arrows to some experimental data points indicate that those are only the lower limits of the decay half-lives determined experimentally. Figure 1 contains the results of the present (MSAFM) theoretical calculations and the data points for carbon-14, oxygen-20, and fluorine-23 cluster emissions. Figures 2, 3, and 4 represent the data and theoretical results of MSAFM calculations for cluster emissions of neon, magnesium, and silicon isotopes, respectively. The decay modes and the experimental values for their half-lives have been presented in Table I. Those data that represent only the lower limits for the decay half-lives have been placed at the bottom. The corresponding results of the present calculations of superasymmetric fission model with microscopic potentials (MSAFM) are also presented along with the results of ASAFM calculations of 1986 [3] and 1991 [4] so as to facilitate the comparison of the results of older calculations [4] with the present one.

The results of the present calculations of the MSAFM have been found to predict the general trend very well for a wide range of experimental data. The quantitave agreement with experimental data for lighter cluster emissions is excellent while that for heavier clusters is reasonable. The degree of reliability of the MSAFM predictions for cluster decay lifetimes are comparable to that of ASAFM [4], although they are not exactly the same. It is worthwhile to mention that all the ASAFM results of 1986 and of 1991 listed in the Table I have been recalculated using zero-point vibration energies given by Eq. (11) of Ref. [3] and Eqs. (5) of Ref. [10], respectively.

The half-lives for cluster radioactivity have been analyzed with microscopic nuclear potentials that are based on profound theoretical basis. The results of the present calculations with MSAFM are in good agreement over a wide range of experimental data and are comparable to the best available theoretical calculations [4] of ASAFM which used parabolic interaction potentials that did not have any microscopic basis. Present calculations certainly put part of the SAFM on a firm theoretical basis. Refinements such as introduction of dissipation while tunneling through the barrier or incorporating the dynamic shape deformations in the density distributions of the clusters may further improve results. It may, however, be realized that as the first illustrative calculations using realistic microscopic cluster interaction potentials, the results of the cluster radioactive decay lifetimes obtained are remarkable. In future, such calculations may therefore be extended to provide reasonable estimates of the lifetimes of nuclear decays by cluster emissions for the entire domain of exotic nuclei.

The author is grateful to Dr. A.K. Chaudhury, Dr. K. Krishan, Dr. S. Bhattacharya, and Dr. J.N. De for many helpful discussions and suggestions.

[1] H.J. Rose and G.A. Jones, Nature (London) **307**, 245 (1984).
[2] D.N. Poenaru and M. Ivascu, J. Phys. (France) **45**, 1099 (1984).
[3] D.N. Poenaru, W. Greiner, K. Depta, M. Ivascu, D. Mazilu, and A. Sandulescu, At. Data Nucl. Data Tables **34**, 423 (1986).
[4] D.N. Poenaru, D. Schnabel, W. Greiner, D. Mazilu, and R. Gherghescu, At. Data Nucl. Data Tables **48**, 231 (1991).
[5] S.S. Malik and R.K. Gupta, Phys. Rev. C **39**, 1992 (1989).
[6] D. N. Poenaru and W. Greiner, *Proceedings of Europhysics International Conference on Rare Nuclear Decays and Fundamental Processes*, Bratislava, Czechoslovakia, 1990; Phys. Scr. **44**, 427 (1991).
[7] G. Shanmugam and G.M. Carmel Vigila Bai, Pramana **53**, 443 (1999).
[8] G. Bertsch, J. Borysowicz, H. McManus, and W.G. Love, Nucl. Phys. **A284**, 399 (1977).
[9] A.K. Chaudhury, D.N. Basu, and B. Sinha, Nucl. Phys. **A439**, 415 (1985).
[10] D.N. Poenaru, W. Greiner, M. Ivascu, D. Mazilu, and I.H. Plonski, Z. Phys. A **325**, 435 (1986).
[11] W. D. Myers and W. J. Swiatecki, Lawrence Berkeley Laboratory Report No. LBL-36803, 1994; Nucl. Phys. **A601**, 141 (1996).
[12] S. Wang, P.B. Price, S.W. Barwick, K.J. Moody, and E.K. Hulet, Phys. Rev. C **36**, 2717 (1987).
[13] R. Bonetti, E. Fioretto, C. Migliorino, A. Pasinetti, F. Barranco, E. Vigezzi, and R.A. Broglia, Phys. Lett. B **241**, 179 (1990).
[14] R. Bonetti, C. Chiesa, A. Guglielmetti, C. Migliorino, A. Cesana, M. Terrani, and P.B. Price, Phys. Rev. C **44**, 888 (1991).
[15] S.P. Tretyakova, S.Y. Zamyatnin, V.N. Kovanstev, S.Y. Korotkin, V.L. Mikheev, and G.A. Timofeev, Z. Phys. A **333**, 349 (1989).
[16] P.B. Price, Nucl. Phys. **A502**, 41C (1989).
[17] A. Sandulescu and W. Greiner, Rep. Prog. Phys. **55**, 1423 (1992).
[18] R. Bonetti, C. Chiesa, A. Guglielmetti, C. Migliorino, P. Monti, A.L. Pasinetti, and H.L. Ravn, Nucl. Phys. **A576**, 21 (1994).
[19] C. Mazzocchi, A. Guglielmetti, R. Bonetti, and R.K. Gupta, Phys. Rev. C **61**, 047304 (2000).